Electron Transfer and Adsorption of Myoglobin on Self-Assembled Surfactant Films: An Electrochemical Tapping-Mode AFM Study

S. Boussaad and N. J. Tao*

Contribution from the Department of Physics, Florida International University, Miami, Florida 33199

Received January 12, 1999

Abstract: We have studied myoglobin (Mb) on graphite basal plane and on self-assembled didodecyldimethylammonium bromide (DDAB) mono- and multilayers with in situ tapping-mode AFM, cyclic voltammetry, and differential capacitance measurements. On graphite, Mb molecules adsorb and aggregate into chainlike features. The aggregation indicates an attractive interaction between the adsorbed molecules. In contrast, the molecules are randomly distributed on the DDAB layers. The adsorption on DDAB changes drastically the domains and defects in the DDAB layers due to a strong Mb−DDAB interaction. On both the bare and the DDAB-coated electrodes, the protein undergoes a fast electron-transfer reaction involving $Fe^{3+} + 1e^- \leftrightarrow Fe^{2+}$ in the heme group. The structure of the DDAB film is potential dependent. At low potentials, the film is in a solidlike phase. When the potential is raised to ∼0 V, the film transforms into a liquidlike phase via a first-order phase transition. The liquidlike phase may be responsible for the fast diffusion of Mb through the DDAB layers.

Introduction

Understanding interactions between proteins and surfaces is critically important in many fields of biomedical science, from biosensors to biocompatible materials.[1,2] In the development of biosensors, for instance, a critical step is to immobilize proteins with intact functions onto the surface of a transducer.[3,4]Although many proteins spontaneously adsorb onto solid surfaces, the adsorbed proteins often denature or adapt undesirable orientations on the surfaces.[5−8] To remedy these problems, many methods have been developed, each with its own advantages and disadvantages.[9]

A widely studied method is to coat an electrode with a layer of organic molecules.[10−13] If appropriate molecules are chosen, the layer can serve both as a cushion that prevents adsorbed proteins from denaturation and as a guide for the proteins to adapt a desirable orientation. A novel extension to this method uses alkylthiol monolayers on Au electrodes.[14,15] The alkylthiols are known to self-assemble into ordered monolayers, with the thiol end anchored onto Au or Ag electrodes.[16] An appropriate functional group on the opposite end can bind a protein, thus immobilizing the protein to the electrode.

More recently, membranes of surfactants[17−23] and natural lipids[24−26] have been used to coat electrodes by self-assembly or Langmuir−Blodgett methods. Because these systems mimic the physiological environment of many membrane-associated proteins, they provide not only an effective way to immobilize proteins onto electrodes for biosensor applications but also nice model systems for studying the biological functions of these proteins. The latter point is important because directly studying proteins in live cells is rather difficult and the model systems allow a variety of powerful techniques, such as atomic force microscopy (AFM), surface plasmon resonance (SPR) spectroscopy, and quartz microbalance, to be used. In this paper, we report a combined in situ tapping-mode AFM and electrochemical study of the structural and electron-transfer properties of myoglobin (Mb) on bare graphite electrode and on didode-

* To whom correspondence should be addressed (e-mail taon@fiu.edu).

(1) Pickup, J. C.; Alcock, S. *Biosens. Bioelectron.* **1991**, *6*, 63.
(2) Chaplin, M. F.; Bucke, C. *Enzyme Technology*; Cambridge University Press: Cambridge, UK, 1990.
(3) Hall, E. A. H. *Biosensors*; Prentice Hall: Englewood Cliffs, NJ, 1991.
(4) Clark, L. C., Jr.; Lyons, C. *Ann. N. Y. Acad. Sci.* **1962**, *102*, 29.
(5) Bowden, E. F.; Hawkridge, F. M.; Blount, H. N. In *Biochemistry*; Srinivasan, S., Ed.; Comprehensive Treatise of Electrochemistry 10; Plenum Press: New York, 1985; p 297.
(6) Heller, A. *Acc. Chem. Res.* **1990**, *23*, 128.
(7) Reed, D. E.; Hawkridge, F. M. *Anal. Chem.* **1987**, *59*, 2334.
(8) Nassar, A. E. F.; Willis, W. S.; Rusling, J. F. *Anal. Chem.* **1995**, *67*, 2386.
(9) Scouten, W. H.; Luong, J. H. T.; Brown, R. S. *Trends Biotechnol.* **1995**, *13*, 178.
(10) Eddowes, M. J.; Hill, H. A. O. *J. Chem. Soc., Chem. Commun.* 1977, 771.
(11) Eddowes, M. J.; Hill, H. A. O. *J. Am. Chem. Soc.* **1979**, *101*, 4462.
(12) Taniguchi, I.; Toyosawa, K.; Yamaguchi, H.; Yasukouch, K. *J. Chem. Soc., Chem. Commun.* **1982**, 1032.
(13) Armstrong, F. A.; Hill, H. A. O.; Walton, N. J. *Acc. Chem. Res.* **1988**, *21*, 407.
(14) Scott, D. L.; Paddock, R. M.; Bowden, E. F. *J. Electroanal. Chem.* **1992**, *341*, 307. Amador, S. M.; Pachence, J. M.; Fischetti, R.; McCauley, J. P.; Smith, A. B.; Blasie, J. K. *Langmuir* **1993**, *9*, 812.
(15) Edmiston, P. L.; Lee, J. E.; Cheng, S.-S.; Saavedra, S. S. *J. Am. Chem. Soc.* **1997**, *119*, 560. Wood.; L. L.; Cheng, S.-S.; Edmiston, P. L.; Saavedra, S. S. *J. Am. Chem. Soc.* **1997**, *119*, 571.
(16) Dubois, L. H.; Nuzzo, R. G. *Annu. Rev. Phys. Chem.* **1992**, *43*, 437.
(17) Cullison, J. K.; Hawkridge, F. M.; Nakashima, N.; Yoshikawa, S. *Langmuir* **1994**, *10*, 877.
(18) Tanaka, K.; Tamamushi, R. *J. Electroanal. Chem.* **1987**, *236*, 305.
(19) Rojas, M. T.; Han, M.; Kaifer, A. E. *Langmuir* **1992**, *8*, 1627.
(20) Kaufmann, J.-M.; Chastel, O.; Quarin, G. *Bioelectrochem. Bioenerg.* **1990**, *23*, 167−172.
(21) Wang, J.; Lu, Z. *Anal. Chem.* **1990**, *62*, 826.
(22) Rusling, J.; Nassar, A.-E. F. *J. Am. Chem. Soc.* **1993**, *115*, 11891.
(23) Nakashima, N.; Masuyama, Mochida, M.; Kunitake, M.; Manabe O. *J. Electroanal. Chem.* **1991**, *319*, 355.
(24) Salamon, Z.; Vitello, L. B.; Erman, J. E. *Bioelectrochem. Bioenerg.* **1989**, *21*, 213.
(25) Salamon, Z.; Hazzard, J. T.; Tollin, G. *Proc. Natl Acad. Sci. U.S.A.* **1993**, *90*, 6420.
(26) Salamon, Z.; Tollin, G. *Biophys. J.* **1996**, *71*, 848.

10.1021/ja990117r CCC: $18.00
Published on Web 04/24/1999

cyldimethylammonium bromide (DDAB) layers self-assembled on the electrode from DDAB vesicle solution.

Mb is a heme protein that functions in both transport and short-term storage of oxygen. The electron-transfer reaction of Mb on electrodes has been studied by several groups.[22,27,28] Rusling and Nassar have studied the reaction on bare and on DDAB-modified pyrolitic graphite electrodes.[22] The DDAB film was cast onto the electrode by placing a drop of DDAB solution onto an abraded graphite and then drying it overnight. The film had an estimated thickness of ~20 μm and was described as a liquid crystalline-like multilayer film with a large amount of water trapped between the layers. Rusling and Nassar found that the protein on the DDAB-coated electrode exhibited a fast electron transfer. The fast electron transfer was attributed to the prevention of impurities from adsorbing onto the electrode by the DDAB film, and to a desirable orientation of the protein in the DDAB film. While the above picture explains many observed features, it does not explain the puzzling observation that the diffusion coefficient of Mb through the DDAB film is nearly as fast as that in bulk solution. We demonstrate here that a combined in situ AFM and electrochemical measurement of Mb on *well-defined* DDAB films prepared by self-assembly can provide new insights into the adsorption of Mb onto the electrodes and useful clues for solving the puzzle.

Experimental Section

ZYH-grade highly oriented pyrolitic graphite (HOPG) from Advanced Ceramics was used as electrodes. Each electrode was cleaved and covered immediately with solution to minimize contamination. Myoglobin from horse skeletal muscle (Fluka) was dissolved in 30 mM tris(hydroxymethyl)aminomethane buffer (Tris-HCl, Fluka) to make a 0.2 mM solution. The buffer contained 50 mM NaBr, and its pH was 7.4. DDAB from Sigma was dissolved in chloroform (ACS reagent and HPLC grade, Sigma) to a concentration of 100 mM. Small unilamellar vesicles of DDAB were prepared by following a simplified method derived from the procedure described in ref 29. In the first step of the preparation, 500 μL of the DDAB solution was added to 50 mL of the Tris-HCl buffer. Then chloroform was evaporated from the aqueous solution by blowing N_2 into the solution for ~30 min, resulting in a 1 mM DDAB solution. To form uniform DDAB vesicles, the mixed solution (DDAB/buffer) was sonicated to clarity in an ice bath for ~40 min.

The AFM experiments were performed with a Nanoscope IIIa multimode SPM (Digital Instrument Inc.). Commercial sharpened Si_3N_4 tips attached to triangular cantilevers were used. The set point was adjusted to minimize the force between the tip and the sample in each measurement. The potential of the graphite electrode was controlled by a Pine Instrument potentiostat (model AFRDE5) with Pt and Ag wires as counter and quasi-reference electrodes, respectively. The Ag quasi-reference electrode was calibrated against a Ag/AgCl electrode (3 M KCl), and all the potentials in this paper are quoted versus Ag/AgCl reference electrode.

The cyclic voltammetry (CV) was measured with an EG&G model 283 potentiostat. A Pt wire and a Ag/AgCl electrode were used as counter and reference electrodes, respectively. For the differential capacitance measurement, an EG&G model 5110 lock-in amplifier interfaced with a PC equipped with a National Instrument data acquisition board was used. Both CV and differential capacitance measurements were carried out in an environmental chamber continuously flushed with N_2.

Results

Mb on HOPG. We have studied Mb adsorption on freshly cleaved HOPG with AFM and cyclic voltammetry. We started the experiment by imaging the HOPG in Tris-HCl buffer and then added a small amount of Mb solution (50 μL) into the buffer while the AFM tip was scanning continuously. Figure 1 shows a sequence of images recorded during the adsorption of the protein. Before addition of Mb into the buffer, the image (Figure 1a) shows a clean HOPG surface in Tris-HCl buffer. Diagonally crossing the image is a surface step which is a common feature on HOPG. After introduction of Mb into the buffer, the image was streaky, which indicates the adsorption of Mb. Slowly (~15 min), the adsorbed Mb began to appear as elongated features (Figure 1b). The elongated features continued to evolve and formed chainlike features (Figure 1c) over time. In about 40 min, a Mb layer, consisting of the chainlike features, was completed (Figure 1d). A typical chain is about 60 nm long and 7 nm wide. Higher resolution images reveal that each chain consists of bloblike features of ~6 nm in dimension (inset of Figure 1d). We believe that each blob is a Mb molecule based on the following two considerations. First, the dimension of the blobs is close to that of Mb determined by X-ray crystallography.[30] Second, the coverage estimated by counting the blobs is about 2×10^{12} cm^{-2}, which agrees well with the coverage determined from the cyclic voltammograms (we will return to this later). The aggregation of Mb into chains indicates an attractive interaction between the adsorbed Mb molecules. In contrast, our previous AFM study found that cytochrome *c*, a similar redox protein, distributed randomly when adsorbed on HOPG surfaces.[31,34] This difference indicates that the attractive interaction does not exist between adsorbed cytochrome *c* molecules. Another difference between Mb and cytochrome *c* is that cytochrome *c* forms a complete layer on HOPG within a few minutes, much quicker than Mb on HOPG. This time difference is not due to a large difference in the adsorption time

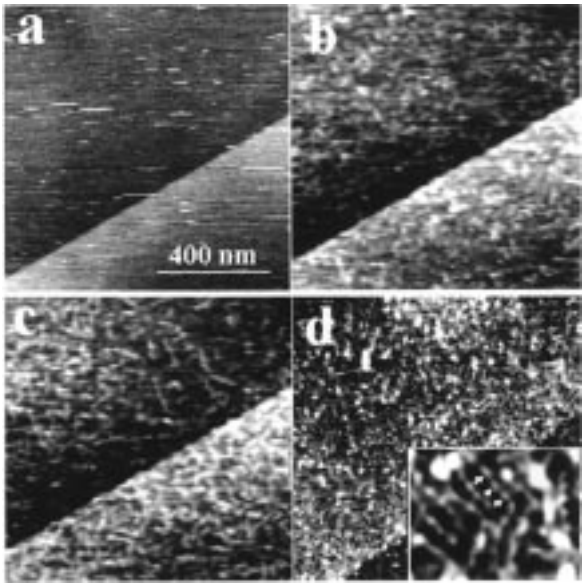

Figure 1. Adsorption of Mb onto bare HOPG revealed by tapping-mode AFM. (a) An image recorded before adsorption, which shows a HOPG surface in Tris buffer. (b and c) Images obtained 15 and 30 min after introduction of Mb into the sample cell, respectively. (d) A complete coverage of Mb on the electrode 45 min after introduction of Mb into the solution. The inset in (d) is a higher magnification image that shows more clearly the chainlike aggregates of Mb.

(27) Cotton, T. M.; Shultz, S. G.; van Duyne, R. P. *J. Am. Chem. Soc.* **1980**, *102*, 7960.

(28) Nassar, A. E. F.; Zhang, Z.; Hu, N.; Rusling, J. F.; Kumosinski, T. F. *J. Phys. Chem. B* **1997**, *101*, 2224.

(29) Barenholz, Y.; Gibbes, D.; Litman, B. J.; Goll, J.; Thompson, T. E.; Carlson, F. D. *Biochemistry* **1977**, *16*, 2806.

(30) Kendrew, J. C.; Bodo, G.; Dintzis, H. M.; Parrish, R. G.; Wyckoff, H.; Phillips, D. C. *Nature* **1960**, *185*, 416.

(31) Boussaad, S.; Tao, N. J.; Arechabaleta, R. *Chem. Phys. Lett.* **1997**, *280*, 397.

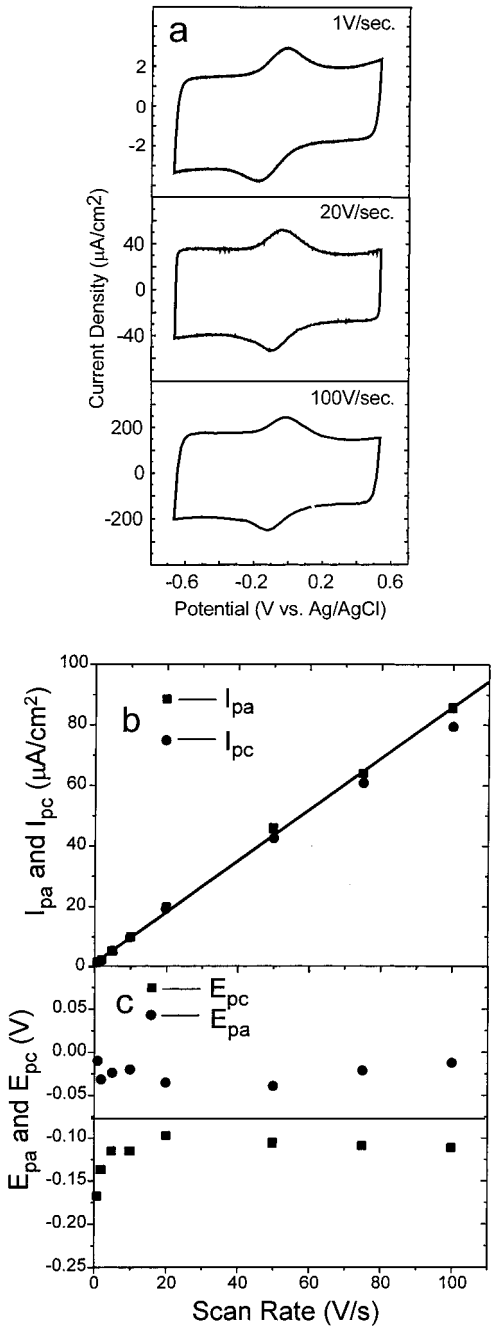

Figure 2. (a) Cyclic voltammograms of Mb adsorbed on bare HOPG at different potential scan rates. (b) The cathodic and anodic peak heights of the redox couple vs scan rate. (c) The cathodic and anodic peak positions of the redox couple vs scan rate.

between the two proteins. In fact, Mb adsorption begins a few minutes after Mb is introduced into the sample cell, but it is initially too mobile to be clearly resolved by AFM. We believe that the much longer time required for the formation of a Mb layer is because the Mb molecules need extra time to rearrange themselves into the chainlike structure that is immobilized for AFM imaging.

The cyclic voltammogram (CV) of the adsorbed Mb shows clearly a pair of peaks corresponding to the reduction and oxidation of Mb (Figure 2a). This is in contrast to the work by Rusling and Nassar, which found no redox peaks in the CV of Mb using a bare graphite electrode.[22] One possible explanation for this discrepancy is that our graphite electrode was a freshly cleaved basal plane of HOPG, while theirs was abraded with sand paper. The abraded graphite electrode exposes a large

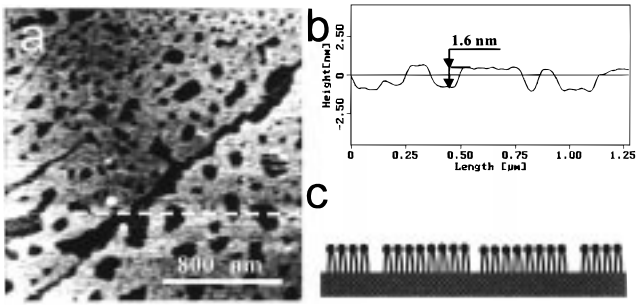

Figure 3. Self-assembled DDAB monolayer on HOPG from a DDAB vesicle solution. (a) Tapping-mode AFM image of the DDAB monolayer in Tris buffer solution. (b) Height profile along the dashed line shown in (a). (c) A model of the DDAB layer that explains the observed images.

fraction of edge plane, which may prevent Mb from forming the stable chainlike features.

Assuming that the electron transfer involves one electron per molecule, the protein coverage from the peak areas in the CV is 1.8×10^{12} cm^{-2}, in good agreement with the AFM images as mentioned before. The coverage is similar to 2×10^{12} cm^{-2}, the coverage for cytochrome *c* on graphite, which is reasonable because of the similarity in the dimensions of the two proteins. The heights of the anodic and cathodic peaks are proportional to the scan rate, which is consistent with the redox of an adsorbed species (Figure 2b). However, the separation between the anodic and cathodic peaks *decreases* initially and then increases as the scan rate increases (Figure 2c). This behavior is not expected for a simple electron transfer of adsorbed species[32] and also is in sharp contrast to the behavior of cytochrome *c* on graphite, which shows a monotonic increase in the peak separation. This abnormal behavior coincides with the formation of Mb aggregates, but further study is needed to elucidate the origin.

Mb on DDAB Layers. After studying Mb on bare HOPG electrode, we turned our attention to Mb on DDAB layers self-assembled on HOPG. We prepared the DDAB layers by exposing the HOPG electrode to the DDAB vesicle solution. The thickness of the DDAB layers was controlled by the amount of the vesicle solution to which the electrode was exposed. We started the experiment by imaging a freshly cleaved HOPG in the buffer solution. After a clear HOPG image was obtained, we introduced various amounts of DDAB solution into the AFM cell. Figure 3a is an image of HOPG in Tris-HCl buffer obtained ~1 h after injecting 25 μL of DDAB vesicle solution into the cell. The image shows a DDAB layer self-assembled on the surface. The layer is rather uniform in thickness but contains many defects or pinholes. The thickness measured from the height profile of the image is about 1.6 nm (Figure 3b), corresponding to a monolayer of DDAB. Because the graphite surface is hydrophobic, the hydrophobic tails of the DDAB molecules likely face the surface while the hydrophilic heads point to the water (Figure 3c). We note that the monolayer is very fragile, and imaging it in contact mode destroys it easily.

We obtained multilayer DDAB films by increasing the amount of DDAB vesicle solution in the AFM cell. Figure 4a is an image obtained ~45 min after introducing 125 μL of DDAB vesicle solution into the sample cell. To estimate the thickness of the film, we zoomed in on a small area and switched to contact mode. After repeatedly scanning the area under a large force in contact mode, we then switched back to tapping mode and zoomed out. The scanning tip swept off the DDAB

(32) Laviron, E. *J. Electroanal. Chem.* **1979**, *101*, 19.

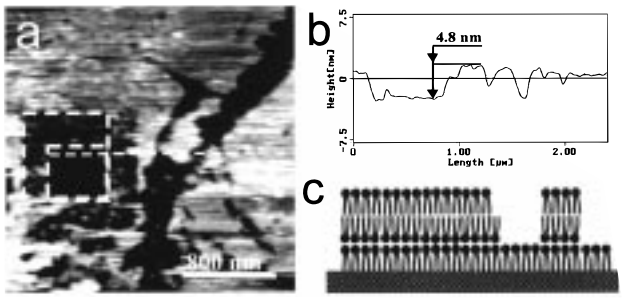

Figure 4. Self-assembled DDAB multilayer on HOPG from a DDAB vesicle solution. (a) Tapping-mode AFM image of the DDAB layer in Tris buffer solution, where the squares outline the regions where the DDAB molecules have been removed with the AFM tip (see text for a more detailed description). (b) Height profile along the dashed line shown in (a). (c) A model of the DDAB layer that explains the observed images.

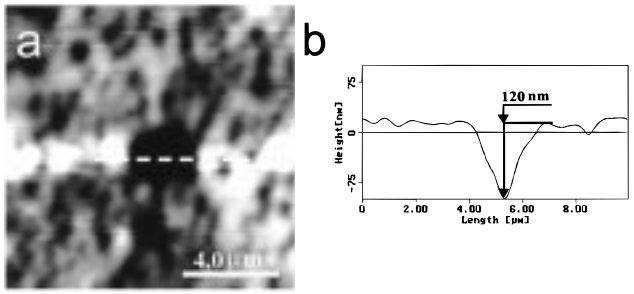

Figure 5. DDAB film cast on HOPG. (a) Tapping-mode AFM image of the DDAB film in Tris buffer solution. The hole near the center of the image was created by removing the DDAB molecules with the AFM tip (see text for a more detailed description). (b) Height profile along the dashed line shown in (a).

molecules and created a square crater in the area. The depth of the crater is ∼4.8 nm (Figure 4b), corresponding to a monolayer plus a bilayer of DDAB (Figure 4c). This observation is consistent with a recent study of lipid vesicles on various electrodes with quartz crystal microbalance (QCM), which found that the vesicles could spread on a hydrophobic surface and formed monolayer and bilayer films.[33]

For comparison, we have also examined the cast films of DDAB prepared using the same procedure as Rusling and Nassar.[22] AFM images of such a cast film show that the cast films were not as uniform as the self-assembled films (Figure 5a). The hole in the middle of the image was created by repeatedly scanning the area in contact mode under a large force. The height profile plot in Figure 5b shows that the hole is 120 nm deep. Since the AFM tip may not penetrate through all the layers, the AFM-measured thickness represents only the minimum thickness of the film. The AFM-tip-created hole was rather stable upon repeated scanning of the area in tapping mode, which means that the film is in a solidlike phase. This appears to contradict a previous differential scanning calorimetry study, which found that the cast DDAB film was in the liquid crystalline phase at room temperature and transformed into the solidlike gel phase below ∼15 °C.[22] One possible explanation is that the AFM reveals only the layers adjacent to the electrode surface, which are, indeed, solidlike. Beyond the solidlike layers are many liquid crystalline-like layers which were measured by the scanning calorimetry but could not be imaged by the AFM. This explanation is supported by the fact that the estimated thickness of the film is 20 μm, much thicker than the 120 nm estimated from the AFM images.

(33) Keller, C. A.; Kasemo, B. *Biophys. J.* **1998**, *75*, 1397.

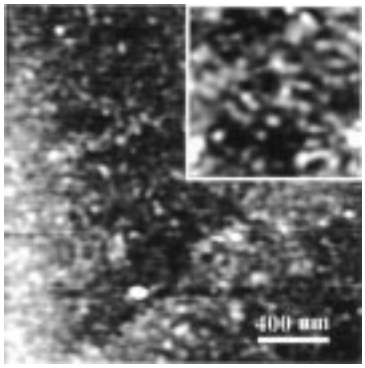

Figure 6. Tapping-mode AFM image of Mb adsorbed onto the DDAB monolayer shown in Figure 3. The inset is a zooming-in image of the adsorbed Mb which shows more clearly the individual Mb molecules as bloblike features.

After studying the DDAB layers, we studied Mb adsorption on them by introducing Mb solution into the AFM cell. Mb adsorbs onto both the DDAB mono- and multilayers and forms a stable monolayer on the surfaces within minutes. Figure 6 is an AFM image of Mb on the DDAB monolayer, which reveals the individual Mb molecules as bloblike features. This is completely different from Mb on bare HOPG electrode, where the Mb molecules aggregate into chainlike structures. This difference can be understood on the basis of the following considerations. On atomically flat HOPG, the adsorbed Mb can diffuse around on the surface more freely and form aggregates. On DDAB surface, however, the adsorbed Mb molecules cannot diffuse freely because of their strong interaction with the DDAB. The interaction with DDAB immobilizes Mb almost immediately upon the adsorption of the protein. This explanation is supported by the following evidence. First, the defects on the DDAB monolayer disappear immediately upon Mb adsorption, which means that the interaction between Mb and DDAB is strong enough to even change the packing of the DDAB monolayer. Second, Mb molecules on the DDAB films can be clearly imaged by AFM immediately after adsorption, while they take nearly 40 min before a stable AFM image can be formed on bare HOPG. On DDAB multilayers, the AFM images of Mb are rather similar to those on the monolayer.

The CV of the adsorbed Mb on the DDAB monolayer reveals a pair of peaks corresponding to the redox reaction of the protein, which is similar to that on bare graphite electrode (Figure 2a). The coverage of Mb obtained from the integrated redox peak areas is $\sim 2.4 \times 10^{12}$ cm^{-2}, which is close to that of a closely packed monolayer of Mb. The peak currents are proportional to the scan rate of the electrode potential, as expected for an adsorbed protein layer (Figure 7a). The separation between the anodic and cathodic peaks is greater than that of Mb on bare graphite, indicating a slower electron transfer. The separation increases as the scan rate increases (Figure 7b), from which the electron-transfer rate is estimated to be about 80 s^{-1}, according to the working curves in ref 32. While the CV for the Mb on DDAB is rather similar to that on bare graphite, the redox potential is shifted negatively by ∼0.05 V for Mb on DDAB (Figures 2c and 7b).

On increasing the thickness of the DDAB layer, the CV becomes more like Mb on the cast film reported by Rusling and Nassar.[22] Figure 8a shows the CV of a multilayer DDAB film at several different scan rates. The thickness of the film estimated from the amount of DDAB and AFM images is ∼15 bilayers. The peak currents increase slower than a linear function of the scan rate, expected for an adsorbed Mb layer, but faster

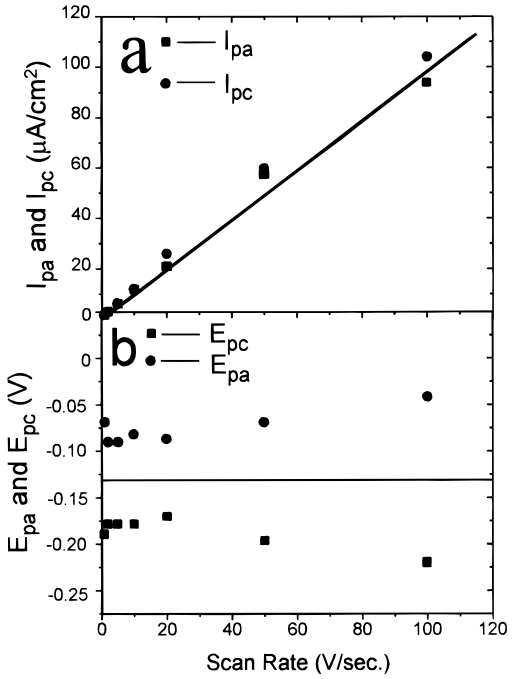

Figure 7. (a) Cathodic and anodic peak heights of the redox couple vs scan rate. (b) Cathodic and anodic peak positions of the redox couple vs scan rate.

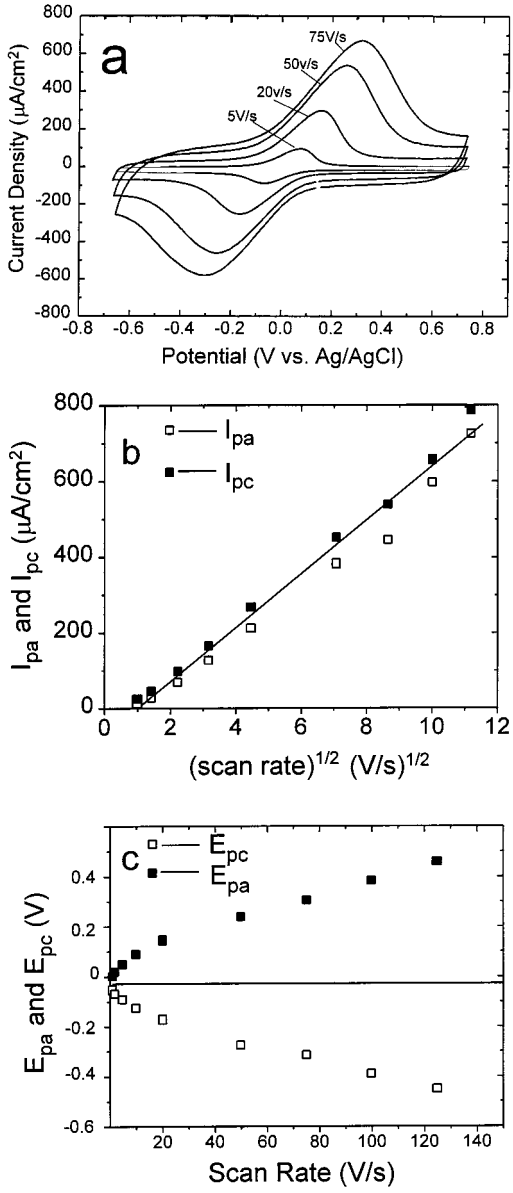

Figure 8. (a) Cyclic voltammograms of Mb adsorbed on DDAB multilayer self-assembled on HOPG at different scan rates. (b) The cathodic and anodic peak heights of the redox couple vs square root of the scan rate. (c) The cathodic and anodic peak positions of the redox couple vs scan rate.

than the square root of the scan rate, expected for a diffusion-limited process (Figure 8b). This behavior can be interpreted in terms of thin-layer electrochemistry. At low scan rates, diffusion is sufficient to bring all the Mb molecules in the thin layer to the electrode surface, and the current is proportional to the scan rate. When the scan rate is fast, the electron transfer becomes diffusion limited, and the current is proportional to the square root of the scan rate. The separation between the cathodic and anodic peaks increases monotonically as the scan rate increases (Figure 8c). Using the peak separations at fast scan rates (>10 V/s) and the diffusion coefficient from ref 22, the electron-transfer rate estimated on the basis of the published curves in ref 35 is about 6×10^{-3} cm/s. This value is in good agreement with the electron-transfer rate reported for Mb in the DDAB film cast on graphite electrodes.[22]

The diffusion coefficient estimated from the CV data is in the order of $10^{-6}-10^{-7}$ cm^2/s, which agrees with the value obtained for the cast film.[22] This value is close to the diffusion of Mb in bulk solution, which is surprising for Mb in a liquid crystalline DDAB film. It is even more puzzling when considering that, near the electrode, the DDAB film is solidlike. Our AFM images show that Mb interacts strongly with the DDAB film upon adsorption and can penetrate into the film, but the diffusion is still expected to be much slower than that in bulk solution.

Dependence of DDAB Structure on the Potential. To resolve this puzzle, we have studied the DDAB film as a function of potential using differential capacitance and AFM. Figure 9 shows a sequence of AFM images of a self-assembled DDAB layer in Tris-HCl buffer obtained at various potentials between −0.4 and 0.4 V. Below ∼0 V, the DDAB film was rather stable and had a thickness of ∼4.8 nm, corresponding to a bilayer on a monolayer (Figure 9a). On increasing the potential to ∼0 V, the image suddenly became streaky, indicating a phase transition in the DDAB film (Figure 9b,c). The streakiness was due to the fact that the film in the new phase was unstable under the scanning tip of AFM, so the new phase is a more liquidlike phase. On increasing the potential to 0.2 V, the image became less streaky and revealed some remaining DDAB molecules on the surface (Figure 9d). The phase transition is fully reversible. On lowering the potential below 0 V, the DDAB film grew back immediately (Figure 9e,f). Because no DDAB was present in the solution, the recovery of the DDAB layer means no desorption took place during the phase transition.

The reversible phase transition is also shown in the differential capacitance data (Figure 10). As the potential increases from negative to positive, the capacitance increases sharply at ∼0.15 V. The capacitance returns to the lower value as the potential is cycled back to negative potentials, but at a more negative potential (∼0.05 V). This hysteresis effect is expected for a first-order phase transition, which has been observed in the phase transition of many interfacial films. For comparison, the

(34) Boussaad, S.; Dziri, L.; Tao, N. J.; Arechabaleta, R.; Leblanc, R. M. *Langmuir* **1998**, *14*, 6215.
(35) Nicholson, R. S. *Anal. Chem.* **1965**, *37*, 1351.

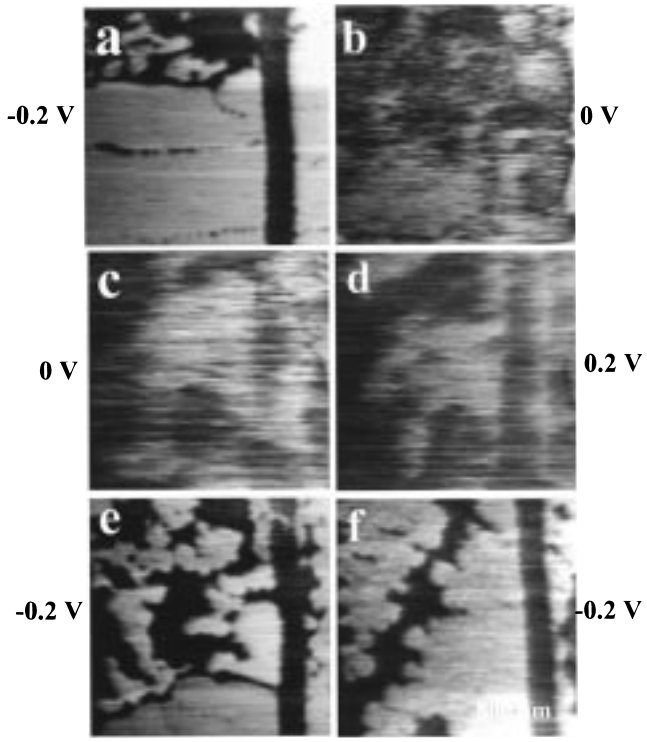

Figure 9. Tapping-mode AFM images of a potential-induced phase transition in the self-assembled DDAB film on HOPG. Images a−f show the DDAB layer at different potentials.

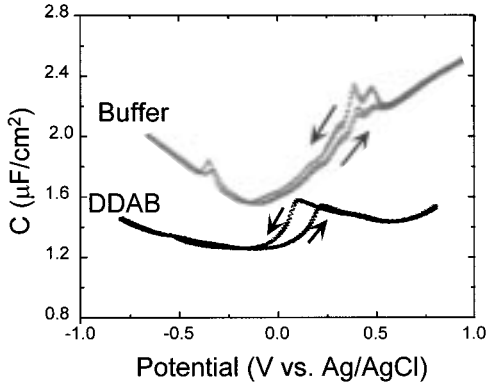

Figure 10. Differential capacitance measurement of the potential-induced phase transition of self-assembled DDAB on HOPG. The stepwise change of the capacitance near 0.1 V is due to the phase transition observed by AFM. For comparison, the capacitance of bare HOPG in the Tris buffer is also shown. The capacitance was measured by superimposing a 38-Hz ac modulation with an amplitude of 10 mV to the electrode potential. The potential was scanned at 0.1 V/s.

differential capacitance of HOPG in the blank buffer solution is also shown in the figure. As expected, the interfacial capacitance in the presence of the DDAB film at negative potentials is smaller than that in the blank buffer solution. After the phase transition, the capacitance increases but is still smaller than the capacitance in the buffer solution. This indicates that the DDAB molecules remain on the electrode surface but with a smaller effective thickness due to, probably, penetration of counterions into the film. This observation is consistent with the AFM images. The phase transition is completely reversible, and the capacitance follows the same hysteresis curve upon repeated cycles of the potential, which means no loss of the DDAB molecules to the bulk solution phase accompanying the phase transition.

In a recent study of Langmuir−Blodgett film of insoluble surfactants on gold electrode, Bizzotto and Lipkowski observed a potential-induced desorption and adsorption of the film.[36−38] Using electroreflectance spectroscopy and light-scattering measurements, they found that the desorbed surfactant molecules form micelles trapped near the electrode surface. In the present system, the potential does not induce desorption of the DDAB film within the studied potential range. Instead, the potential induces a phase transition from the solidlike bilayer phase at low potentials to a liquidlike phase at high potentials. This reversible phase transition may be triggered by the electrostatic interaction between the charged electrode surface and the positively charged headgroup of DDAB, which changes from attractive at low potentials to repulsive at positive potentials.

For a complete understanding of this phase transition, further study is needed. Nevertheless, the observation of the phase transition provides an explanation of the unusually high diffusion coefficient of Mb through the DDAB film based on the following consideration. Mb diffusion in the solidlike layers is slow, but, when the potential is cycled to positive potentials, the layers transform into the liquidlike phase through which Mb diffuses quickly to the electrode surface. Another factor that enhances the transport is the strong interaction between Mb and DDAB, which allows the individual Mb molecules to penetrate into the DDAB film.

Conclusions

Mb spontaneously adsorbs onto freshly cleaved HOPG and forms a monolayer in which the individual Mb molecules aggregate into a chainlike structure. The aggregation indicates an interaction between the adsorbed Mb molecules. The adsorbed Mb undergoes a fast electron-transfer reaction, corresponding to $Fe^{2+} + 1e^- \leftrightarrow Fe^{3+}$. The coverage of the adsorbed Mb determined from the total amount of charge transfer is in good agreement with the AFM images.

Mb also spontaneously adsorbs onto the DDAB layers self-assembled on the HOPG. The adsorption changes dramatically the defects in the DDAB film, indicating a strong interaction between Mb and DDAB. Instead of forming the chainlike aggregates, Mb molecules are randomly distributed on the DDAB. The adsorbed Mb exhibits a pair of peaks in the CV, corresponding to the electron-transfer reaction. The characteristics of the CV depend on the thickness of the DDAB film. On a thin DDAB film, the CVs can be described in terms of an adsorbed species, similar to that of Mb on bare HOPG. On a thick DDAB film, the CV has the characteristics of a diffusion-limited process, similar to that of cast DDAB film reported in the literature.[22]

The DDAB film is not stable at all potentials. At low potentials, the DDAB appears to be solidlike, as judged by the well-defined domain boundaries and defects. Increasing the potential triggers a phase transition, transforming the solidlike phase into a liquidlike phase. This phase transition may explain the unusually fast diffusion of Mb in the DDAB film extracted from the CVs.

Acknowledgment. Financial support is acknowledged through grants from the NIH (GM-08205) and AFSOR (F49620-96-1-0346).

JA990117R

(36) Bizzotto, D.; Lipkowski, J. *J. Electroanal. Chem.* **1996**, *409*, 33.
(37) Bizzotto, D.; Noel, J. J.; Lipkowski, J. *Thin Solid Films* **1994**, *248*, 69.
(38) Bizzotto, D.; Lipkowski, J. *Prog. Surf. Sci.* **1995**, *50*, 237.